CHEMISTRY OF MATERIALS
Article

Chem. Mater. **2010,** *22,* 2375–2383 2375
DOI:10.1021/cm903659g

Cd Substitution in $M_xZn_{4-x}Sb_3$: Effect on Thermal Stability, Crystal Structure, Phase Transitions, and Thermoelectric Performance

Birgitte L. Pedersen,[†] Hao Yin,[†] Henrik Birkedal,[†] Mats Nygren,[‡] and Bo B. Iversen*,[†]

[†]*Centre for Materials Crystallography, Department of Chemistry and iNANO, Aarhus University, Langelandsgade 140, DK-8 Aarhus C, Denmark, and* [‡]*Department of Inorganic Chemistry, Stockholm University, SE-10691 Stockholm, Sweden*

Received December 4, 2009. Revised Manuscript Received February 5, 2010

The effects of Cd substitution in $M_xZn_{4-x}Sb_3$ on the high-temperature thermal stability, low-temperature phase transitions and thermoelectric properties have been studied on three samples with a substitution degree of 0.1, 1, and 2 at % Cd (x = 0.004, 0.04, 0.08). The high-temperature thermal stability in atmospheric air of a 1% substituted sample is compared with an unsubstituted Zn_4Sb_3 sample. Multitemperature synchrotron powder diffraction data reveals that while only ~42 wt % of the original Zn_4Sb_3 phase remains in the unsubstituted sample after three heating cycles to 625 K, 78 wt % is preserved in the Cd-substituted sample. Thus, Cd-substitution provides a significant improvement of the thermal stability of Zn_4Sb_3. Multitemperature synchrotron powder diffraction data measured between 90 and 300 K reveal that Cd substitution has a suppressing effect on the $\alpha'-\alpha-\beta$ phase transitions. With increasing substitution, there is also a significant change in the individual Zn site occupancies. Differential scanning calorimetry shows an apparent correlation between Cd content and phase transition temperature. Thermoelectric properties have been measured from 2 to 400 K for all samples, and although some physical properties are significantly affected by doping, no immediate improvement of ZT was achieved.

Introduction

The β-phase of the p-type semiconductor Zn_4Sb_3 is an excellent thermoelectric material in the intermediate temperature range (473−673 K).[1,2] Even though intensive research in recent years has resulted in complex materials such as LAST and SALT compounds with superior thermoelectric performance to Zn_4Sb_3 in this temperature range,[3,4] the fundamental attractiveness of Zn_4Sb_3 remains unchallenged. Thus, Zn_4Sb_3 is probably the cheapest thermoelectric material known, and it is made of nontoxic elements. These are very important points for potential commercial applications.

The thermoelectric properties of a material can be summarized in the dimensionless thermoelectric Figure of Merit defined as $ZT = TS^2/\rho\kappa$, where S is the Seebeck coefficient, ρ the electrical resistivity, κ the thermal conductivity, and T the absolute temperature. The thermal conductivity consists of a lattice part (κ_L) and an electronic part (κ_e). It is the extremely low lattice contribution to the thermal conductivity that gives β-Zn_4Sb_3 a high ZT.[1] However, the real ZT value of Zn_4Sb_3 materials is a tricky point because it has been found that Zn_4Sb_3 decomposes at temperatures below the expected stability range forming ZnSb and elemental Zn as decomposition products.[1,5,6] Typically, ZT values are reported on the basis of individual measurement of S, σ and κ. However, since the material decomposes and thereby attains a drastic reduction in the figure of merit,[7] the reported values are often based on measurements carried out on different samples. Because of the degradation, multiplication of values measured on different samples during different measurements does not give a reliable picture of the thermoelectric performance of the material. When thermally cycled, the ZT values of β-Zn_4Sb_3 are reduced from a maximum of about 1.2 to below 0.5.[7] It is therefore of high interest to find ways to stabilize Zn_4Sb_3 at elevated temperatures. This can be done by employing a zonemelting technique, where the samples show a drastically reduced tendency to thermal degradation.[8] It would, however, be desirable if alternative ways could be found based on the simpler quench synthesis method. Here, we explore if Cd substitution is a possible route to achieve this goal.

Significant effort has been put into further improving the thermoelectric performance of Zn_4Sb_3 by atomic substitution, especially since the report from Borshchevsky

*Corresponding author. Tel: +45 89423969. E-mail: bo@chem.au.dk.

(1) Caillat, T.; Fleurial, J. P.; Borshchevsky, A. *J. Phys. Chem. Solids* **1997**, *58*, 1119.
(2) Caillat, T.; Borshchevsky, A.; Fleurial, J.-P. U.S. Patent 6 942 728 B2, **2005**.
(3) Sootsman, J. R.; Chung, D. Y.; Kanatzidis, M. G. *Angew. Chem.* **2009**, *48*, 8616.
(4) Snyder, G. J.; Toberer, E. S. *Nat. Mater.* **2008**, *7*, 105.
(5) Mozharivskyj, Y.; Janssen, Y.; Harringa, J. L.; Kracher, A.; Tsokol, A. O.; Miller, G. J. *Chem. Mater.* **2006**, *18*, 822.
(6) Zhang, L. T.; Tsutsui, M.; Ito, K.; Yamaguchi, M. *J. Alloys Compd.* **2003**, *358*, 252.
(7) Iversen, B. B.; Lundtoft, B.; Christensen, B.; Platzek, D. WO Patent No. 128 467, **2006**.
(8) Pedersen, B. L.; Iversen, B. B. *Appl. Phys. Lett.* **2008**, *92*, 161907.

Published on Web 02/25/2010

et al. showed an improved thermoelectric performance of Cd-substituted Zn_4Sb_3 samples.[9] That investigation included a sample with stoichiometry $Zn_{3.2}Cd_{0.8}Sb_3$, which had a figure of merit reaching 1.4 at 523 K in the first thermal cycle. Many investigations have been carried out on the properties of Cd_4Sb_3, which has an analogous structure to Zn_4Sb_3.[10,11] There has been some discussion about the solid-solution range of $Cd_4Sb_3-Zn_4Sb_3$. Record et al. found the solubility of Cd in Zn_4Sb_3 to be ~43 at %, giving a maximum formal stoichiometry of $Zn_{2.28}Cd_{1.72}Sb_3$, whereas Nakamoto et al. reported a maximum Cd stoichiometry of $Zn_{2.4}Cd_{1.6}Sb_3$.[12,13] A solubility of 50 at % has also been reported by Ohtaki et al. using the vacuum casting method without annealing.[14] However, a study by Kuznetsov et al. showed a maximum Cd stoichiometry of only $Zn_{3.76}Cd_{0.24}Sb_3$.[15] It would be fair to say that the quality of the reported powder X-ray diffraction (PXRD) data vary a lot between different studies, and in some cases PXRD data are not even included to show that phase pure materials are available and to substantiate the claims of the stoichiometry. From the published PXRD data, it is clear that not all the reported samples are phase pure. In the present study, we limit ourselves to small doping levels, because only for these levels have we been able to obtain completely phase-pure samples as measured by synchrotron powder X-ray diffraction, which typically allows detection of impurity phases down to 0.1%.[16] Another reason for limiting the amount of Cd substitution is that theoretical calculations done by Cargnoni et al. on the defect structure revealed by X-ray diffraction suggested that the electronic properties of the Zn_4Sb_3 structure would be very sensitive to a light doping of the unit cell.[17] They predicted that adding 0.33 extra electrons per unit cell would cause an increase in the Seebeck coefficient to about 260 μV/K, which is approximately twice the value for pure Zn_4Sb_3.[1]

The outstanding thermoelectric properties of Zn_4Sb_3 are believed to originate from the presence of three interstitial zinc sites, which create a disordered crystal structure and effectively lowers the thermal conductivity while preserving the electrical conductivity.[17,18] When the temperature is lowered from ambient, the crystal structure goes through two phase transitions, $\beta \rightarrow \alpha$ and $\alpha \rightarrow \alpha'$, before eventually reaching an ordered triclinic α'-phase at ~230 K.[5] In the α'-phase, the Zn interstitials become part of the crystalline network.[19,20] In the present study, we also examine the effect of Cd substitution on the crystal structure and the low-temperature phase transitions

Experimental Section

Synthesis. For the investigation of the effect of Cd-doping on the low-temperature phase transitions and physical properties, a total of four samples were synthesized, $Cd_xZn_{4-x}Sb_3$, $x = 0$, 0.004, 0.04, 0.08. At a later point, two additional samples ($x = 0$ and 0.04) were synthesized to investigate the high temperature thermal stability. All samples were prepared from stoichiometric ratios of 99.99% zinc shots, 99.5% antimony powder, and 99.99% cadmium powder. The elements were weighed in stoichiometric ratios in a quartz ampule, which was evacuated and sealed. After sealing, the ampule was placed horizontally in a tube furnace, and heated with a 400 K/h ramp to 973 K under continuous rotation. The sample was held at this temperature for 2 h before quenching in ice water. This resulted in a polycrystalline solid, which was ground in an agate mortar to give a homogeneous powder. To ensure that the sample was single phase PXRD data were recorded using CuK_α radiation in a 2θ-range of 8−84° with a Stoe STADI P diffractometer.

Synchrotron Powder Diffraction. High-resolution multitemperature synchrotron PXRD data were recorded below room temperature on three of the samples from the first synthesis batch (unsubstituted Zn_4Sb_3, $Cd_{0.04}Zn_{3.96}Sb_3$ and $Cd_{0.08}Zn_{3.92}Sb_3$), using the large Debye−Scherrer camera at beamline BL02B2, SPring8, Japan.[21] High-temperature (300−625 K) synchrotron PXRD data were recorded at the same beamline on the two samples from the second synthesis batch (unsubstituted Zn_4Sb_3 and $Cd_{0.04}Zn_{3.96}Sb_3$).

A homogeneous grain size is important for measuring high quality PXRD data. Thus, the samples were sieved (45 μm), and only the smaller crystallites were used. The powders were then floated with ethanol in a Petri dish, and left for sedimentation. After 1 min, the top layer of the ethanol was removed into a new Petri dish, and left for further sedimentation for five minutes. The top layer was again removed into a new Petri dish and the ethanol was evaporated, leaving a sample fraction of homogeneous grain size. The samples were transferred to 0.2 mm capillaries, and held in an ultra sound bath for about 5 min to obtain a dense packing of the powders.

In the low-temperature synchrotron powder diffraction experiment, long exposure data sets (65 min) were recorded with $\lambda = 0.420998(3)$ Å at 300 and 180 K. The wavelength was determined by calibration with a CeO_2 standard. Multi temperature diffraction data in the range of 180−290 K, $\Delta T = 10$ K, were recorded with 7 min exposure time at the same wavelength. All data sets were Rietveld refined with the program FULLPROF,[22] using a pseudo Voigt profile function, and a background modeled with linear interpolation between approximately 65 points. The structural model of Snyder et al.[18] was used as starting model for the β-phase refinements. Two series of

(9) Caillat, T.; Borshcevsky, A.; Fleurial, J.-P. High-Performance Thermoelectric Materials Based on β-Zn_4Sb_3. NASA Tech Briefs; National Aeronautics and Space Administration: Washington, D.C., **1999**.
(10) Tengå, A.; Lidin, S.; Belieres, J.-P.; Newman, N.; Wu, Yang.; Häussermann, U. *J. Am. Chem. Soc.* **2008**, *130*, 15564.
(11) Liu, Y.; Tedenac, J.-C. *CALPHAD: Comput. Coupling Phase Diagrams Thermochem.* **2009**, *33*, 684.
(12) Nakamoto, G.; Souma, T.; Yamaba, M.; Kurisu, M. *J. Alloys Compd.* **2004**, *377*, 59.
(13) Record, M. C.; Izard, V.; Bulanova, M.; Tedenac, J. C. *Intermetallics* **2003**, *11*, 1189.
(14) Souma, T.; Ohtaki, M. *J. Alloys Compd.* **2006**, *413*, 289.
(15) Kuznetsov, V. L.; Rowe, D. M. *J. Alloys Compd.* **2004**, *372*, 103.
(16) Johnsen, S.; Bentien, A.; Madsen; Georg, K. H.; Nygren, M.; Iversen, B. B. *Phys Rev B.* **2007**, *76*, 245126.
(17) Cargnoni, F.; Nishibori, E.; Rabiller, P.; Bertini, L.; Snyder, G. J.; Christensen, M.; Gatti, C.; Iversen, B. B. *Chem.—Eur. J.* **2004**, *10*, 3862.
(18) Snyder, G. J.; Christensen, M.; Nishibori, E.; Caillat, T.; Iversen, B. B. *Nat. Mater.* **2004**, *3*, 458.
(19) Mikhaylushkin, A. S.; Nylen, J.; Haussermann, U. *Chem.—Eur. J.* **2005**, *11*, 4912.
(20) Nylen, J.; Andersson, M.; Lidin, S.; Haussermann, U. *J. Am. Chem. Soc.* **2004**, *126*, 16306.
(21) Nishibori, E.; Takata, M.; Kato, K.; Sakata, M.; Kubota, Y.; Aoyagi, S.; Kuroiwa, Y.; Yamakata, M.; Ikeda, N. *J. Phys. Chem. Solids* **2001**, *62*, 2095.
(22) Rodríguez-Carvajal, J. *FULLPROF 2000*; Institut Laue-Langevin: Grenoble, France, 2001

Table 1. Selected Details from Rietveld Refinement of the α Phase at 190 K, and the *β* Phase at 290 K for the Unsubstituted and Cd-Substituted Samples, Respectively;. *X* and *Y* are the Lorentzian FWHM Parameters Corresponding to Size and Strain Broadening, Respectively

samples	unsubstituted	$Cd_{0.04}Zn_{3.96}Sb_3$	$Cd_{0.08}Zn_{3.92}Sb_3$
	α Phase at 190 K		
t_{Exp} (min)	7	7	7
no. of points	3295	3295	3295
no. of reflns	13731	13758	13638
no. of params	70	91	91
R_F (%)	1.35	2.63	2.61
R_{Bragg} (%)	2.70	3.91	5.78
R_p (%)	3.59	4.26	5.62
R_{wp} (%)	4.87	5.56	8.21
χ^2	11.3	12.4	35.00
a (Å)	17.4077(5)	17.4204(7)	17.4281(7)
b (Å)	17.3906(8)	17.3825(6)	17.3827(6)
c (Å)	10.8545(4)	10.8755(4)	10.8788(3)
α (deg)	81.565(2)	81.572(2)	81.567(2)
β (deg)	81.511(2)	81.513(2)	81.519(2)
γ (deg)	41.134(2)	41.131(2)	41.125(2)
X	0.282(5)	0.227(6)	0.1474(8)
Y	0.0126(6)	0.0167(5)	0.0268(6)
V (Å^3)	2134.7(1)	2139.31(1)	2140.68(1)
	β Phase at 290 K		
t_{Exp} (min)	7	7	7
no. of points	7516	7516	7515
no. of reflections	4923	4910	4910
no. of parameters	78	85	84
R_F (%)	1.42	1.91	1.74
R_{Bragg} (%)	2.87	2.99	2.65
R_p (%)	3.25	3.3	2.91
R_{wp} (%)	4.53	4.52	4.04
χ^2	10.9	11.1	8.57
a = *b* (Å)	12.2257(1)	12.2334(1)	12.2436(1)
c (Å)	12.4152(1)	12.4244(1)	12.4333(1)
X	0.262(5)	0.247(4)	0.237(4)
Y	0.0150(5)	0.0137(4)	0.0140(4)
B_{iso} Sb1	1.207(28)	1.29(3)	1.249(3)
B_{iso} Sb2	1.050(28)	0.96(3)	1.004(3)
B_{iso} Zn	1.789(52)	1.41(5)	1.445(5)
occ Zn1	0.903(3)	0.852(4)	0.855(4)
occ Zn2	0.060(1)	0.044(1)	0.047(1)
occ Zn3	0.060(1)	0.098(3)	0.102(3)
occ Zn4	0.057(2)	0.057(2)	0.057(2)
V (Å^3)	1607.08(2)	1610.27(3)	1614.11(3)

refinements were carried out on the multitemperature data; one refining the α-phase moving up in temperature, and one refining the *β*-phase moving down in temperature. The structure of Nylén et al.[20] was used for refining the α/α′-phase. Because of the complex structure, it was necessary to restrict the data set to $2\theta < 35°$ in the α-phase refinements, because the maximal number of reflections allowed in FULLPROF was exceeded. For the same reason, refinements were limited to background, zero point, lattice constants, profile parameters, and atomic positions. Atomic displacement parameters (ADPs) at a given temperature were estimated by linear extrapolation from the results of the multitemperature *β*-phase refinements.[23]

In the high temperature synchrotron powder diffraction experiment, data were recorded at $\lambda = 0.422359(2)$ Å with an exposure time of 5 min. Data sets were recorded at 300, 400, 500, 505, 510, 515, 520, 525, 530, 535, 540, 575, and 625 K. Furthermore, three heating cycles (300 K → 625 K → 300 K → 625 K → 300 K → 625 K → 300 K) were performed to investigate the stability in a realistic environment, i.e., heating and cooling of a thermoelectric device in atmospheric air. All data sets have been

(23) Pedersen, B. L.; Birkedal, H.; Nygren, M.; Frederiksen, P. T.; Iversen, B. B. *J. Appl. Phys.* **2009**, *105*, 013517.

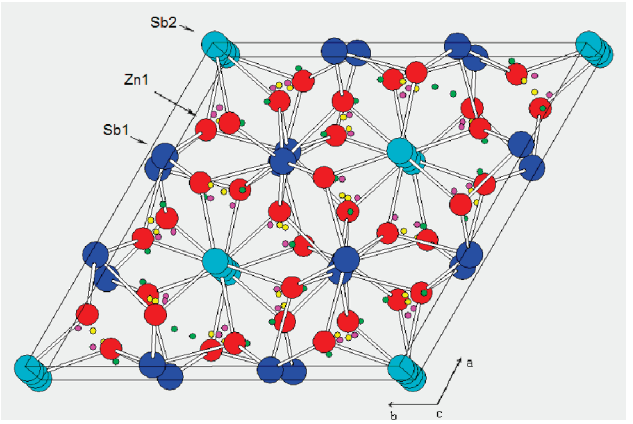

Figure 1. Crystal structure of Zn_4Sb_3. Sb sites and Zn1 site are shown as marked. Interstitial Zn2, Zn3, Zn4 sites are shown in small green, purple, and yellow balls, respectively.

Rietveld refined against the model of Snyder et al.[18] as described above.

Thermal Analysis. Differential scanning calorimetry (DSC) was performed on a Netzsch STA 449 C using Al crucibles with pierced lids and a heating/cooling rate of 10 K/min. The experiments were performed in He atmosphere using gaseous nitrogen for cooling rather than liquid nitrogen since this resulted in more stable conditions and greatly facilitated the measurements of the very weak DSC signals associated with the phase transitions. The instrument was calibrated against the melting points of Hg, In, Sn, Bi, Zn, and C_6H_{12} before use.

Transport Properties. Transport properties were measured on pellets compacted by Spark Plasma Sintering (SPS) with compaction parameters of $T = 673$ K and $P = 100$ MPa. Compaction times were 300 s for the three Cd-substituted samples, and 60 s for the unsubstituted sample. The Thermal Transport Option (TTO) of a Quantum Design PPMS was used to measure the Seebeck coefficient, thermal conductivity and resistivity using a four-probe lead configuration and silver filled epoxy glue contacts.

Results and Discussion

Low-Temperature Synchrotron Powder Diffraction. To study the effect of Cd doping in the crystal structure, multitemperature synchrotron powder diffraction data are used to examine the α′−α−*β* phase transitions. Selected crystallographic data and details of the α′/α and *β*-phase multitemperature synchrotron powder refinements are given in Table 1 and the supporting material. A structural drawing of the *β*-phase with atomic numbering is shown in Figure 1. Observed and calculated diffraction patterns for the α-phase (190 K) and the *β*-phase (290 K) are included in the Supporting Information.

In the refinements and theoretical calculations done by Cargnoni et al.,[17] the occupancy of the interstitial Zn2 and Zn3 sites were constrained to be identical. This constraint was kept in the initial refinement of the *β*-phase. The initial refinements performed with constrained Zn2 and Zn3 occupancies revealed an increased Zn content compared with previously reported stoichiometries. Calculating the stoichiometry based on the refined occupancies in the 300 K data set gave a stoichiometry of $Zn_{39.1(1)}Sb_{30}$

and $Zn_{39.0(1)}Sb_{30}$ for $Cd_{0.08}Zn_{3.92}Sb_3$ and $Cd_{0.04}Zn_{3.96}Sb_3$, respectively. Although different samples may have slightly different Zn occupancies, it is unlikely to reach the full formal Zn occupancy ($Zn_{39}Sb_{30}$) since Zn_4Sb_3 is reported to be a *p*-type semiconductor, and it is therefore expected to be cation-poor.[18] Reaching a higher Zn content would mean that the sample would be an *n*-type semiconductor, which is in contradiction to the measured thermopower of the sample (see below). The increased Zn occupancy strongly indicates that the more electron rich atom Cd has partly substituted for Zn in the structure. To better examine the Cd substitution, the occupancy constraint was removed in the subsequent refinements and the occupancies were refined independently for all four Zn sites. Removing the occupancy constraint lowered χ^2 from 68.3 to 61.3 and R_F from 2.97 to 2.79 for $Cd_{0.08}Zn_{3.92}Sb_3$, thereby giving a much better fit (see the Supporting Information). Interestingly, refining the Zn occupancies independently give rise to a shift in specific site occupancies compared with the values reported by Snyder et al.[18] In that model, the main Zn1 framework site is ~89% occupied and the three interstitial sites are each ~5% occupied, but the refined occupancy of both Cd-substituted samples consistently showed a lower framework occupancy of only ~84%. The "missing" Zn was found on the interstitial Zn3 site, which had an increased occupancy of ~10%. The analogous Cd_4Sb_3 compound has been investigated by Zelinska et al.[24] They found that Cd_4Sb_3 crystallizes in the same space group and displays the same main sites as Zn_4Sb_3 but has five interstitial Cd sites in contrast to the three sites in the Zn compound. As in Zn_4Sb_3, the sites are only partly occupied, with the main site having an occupancy of ~82%, and the five interstitial sites having occupancies of ~2−7%. The present refined occupancy on the main site is closer to the value for Cd_4Sb_3 given by Zelinska,[24] than it is to the reported occupancy of the main site in Zn_4Sb_3.[18] This suggests that introducing even small amounts of Cd in Zn_4Sb_3 changes the structure toward that of pure Cd_4Sb_3. The stoichiometry calculated from the refinements are $Zn_{37.8(2)}Sb_{30}$ and $Zn_{38.2(2)}Sb_{30}$ for $Cd_{0.08}Zn_{3.92}Sb_3$ and $Cd_{0.04}Zn_{3.96}Sb_3$, respectively. Because the increase in occupancy consistently takes place on the Zn3 site, this could indicate the presence of Cd on this site. To test this, a number of refinements were carried out using the same refinement strategy as used for detecting slight Hg substitution in Zn_4Sb_3.[25] In all cases, the Cd occupancy refined to negative values indicating that no Cd is present on the interstitial sites. However, this does not necessarily imply that Cd substitution did not take place; merely that for Cd with less scattering contrast compared with Hg, the data at hand do not allow direct detection of the specific location in the structure.

The cell parameters *a* and *c* for $Cd_{0.04}Zn_{3.96}Sb_3$ and $Cd_{0.08}Zn_{3.92}Sb_3$ and the unsubstituted reference sample

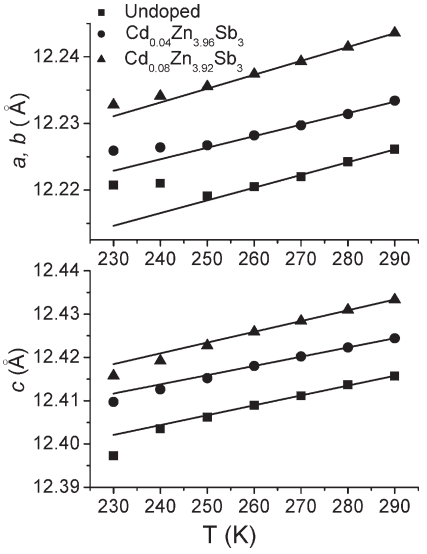

Figure 2. Top: *a*, *b*-axis as a function of temperature for unsubstituted and Cd-substituted samples. Bottom: *c* -axis as a function of temperature for unsubstituted and Cd-substituted samples. All values derived from Rietveld refinement. The standard deviation for each point is below 0.0003 Å. Lines represent straight line fits to the four highest temperatures.

are shown as a function of temperature in Figure 2. For the *a*-axis (Figure 2a), all three samples display the same decreasing behavior down to 250 K. At 250 K, the α/β phase transition is indicated by an increase of the *a*-axis for the unsubstituted sample, whereas the 1 and 2 at % Cd sample show progressively smaller effects as can be seen by comparing with extrapolations of linear fits to the four highest temperature data points. In case of the *c*-axis (Figure 2b) the same picture emerges, but now the effect of the phase transition is a decrease. Both the *a* and *c*-axes show a significant increase in the β-phase as a result of Cd doping. Linear fits to the four high temperature points provide estimates of the coefficient of thermal expansion, which in all cases is found to be smaller for the *a*- than for the *c*-axis (for example $15.7(8) \times 10^{-6}\,K^{-1}$ versus $18.5(5) \times 10^{-6}\,K^{-1}$ for the *a*- and *c*-axes, respectively) and does not display a clear dependence on Cd-content. The lattice parameters given in Table 1 clearly suggest that there is a relationship between the doping level of Cd and the increase in *a*- and *c*-axes. A linear relationship has been observed by other authors in samples with much higher doping degree,[12,14,15] and a solid solution up to $Zn_2Cd_2Sb_3$ has been proposed on that basis.[14] However, the values of the lattice constants for unsubstituted samples reported in the literature are somewhat higher than observed in this study making direct comparison difficult.[12,14,15] Although the Cd atoms could not be located in the structure by Rietveld refinement, the changes in lattice parameters strongly indicate that Cd has been substituted into the structure.

The low-temperature phase transitions have been modeled from the multitemperature diffraction data. All data sets were modeled with a Pseudo-Voigt peak shape function, and the integral breadth was subsequently calculated and normalized to the 290 K value. A phase transition can

(24) Zelinska, O. Y.; Bie, H. Y.; Mar, A. *Chem. Mater.* **2007**, *19*, 1518.
(25) Pedersen, B. L.; Birkedal, H.; Nishibori, E.; Bentien, A.; Sakata, M.; Nygren, M.; Frederiksen, P. T.; Iversen, B. B. *Chem. Mater.* **2007**, *19*, 6304.

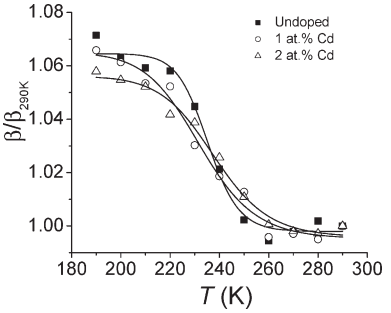

Figure 3. Integral breadth normalized to 290 K value as a function of temperature for unsubstituted Zn_4Sb_3 (full squares), $Cd_{0.04}Zn_{3.96}Sb_3$ (open circles), and $Cd_{0.08}Zn_{3.92}Sb_3$ (open triangles). The trend has been modeled with a sigmoidal function.

often be detected by peak-splitting and appearance of additional peaks, but the complex structure of Zn_4Sb_3 gives rise to approximately 5000 and 13 000 peaks within our data range in the β- and α-phases, respectively. This means that the α-phase peaks are very close to the 2θ position of the β-phase peaks, and an effective peak broadening is observed instead of peak splitting. Figure 3 shows the integral breadth of reflection (300) (as indexed in the β-phase) as a function of temperature for unsubstituted Zn_4Sb_3, $Cd_{0.04}Zn_{3.96}Sb_3$, and $Cd_{0.08}Zn_{3.92}Sb_3$, normalized to the 290 K value. The trend of peak broadening has been modeled by a sigmoidal function. When moving downward in temperature, the unsubstituted sample displays an increase in integral breadth starting at 250 K and ending at 220 K, indicating that the phase transitions take place in this temperature interval. This is consistent with the phase transition temperature of 254 K for polycrystalline samples reported by Mozharivskyj et al.[5] For the two Cd-substituted samples, the increase begins at 260 K and ends at 220 and 210 K for $Cd_{0.04}Zn_{3.96}Sb_3$ and $Cd_{0.08}Zn_{3.92}Sb_3$, respectively, suggesting that the phase transition is taking place over a slightly larger temperature span. The temperature resolution of the experiment (10 K) does not permit for detecting the presence of two distinct phase transitions, $\beta \rightarrow \alpha$, $\alpha \rightarrow \alpha'$.

High-Temperature Synchrotron Powder Diffraction. To study the effect of slight Cd-doping on the thermal stability of Zn_4Sb_3, Rietveld refinement of high temperature synchrotron powder diffraction data is used to identify and quantify the decomposition products generated during heating of the samples from the second synthesis batch (unsubstituted and $Cd_{0.04}Zn_{3.96}Sb_3$). Refinement of the 300 K data sets measured before heating reveal that both samples are extremely phase pure, and impurity phases therefore cannot significantly influence the decomposition. Observed and calculated diffraction patterns before and after heating at 300 K are shown in Figure 4 for unsubstituted Zn_4Sb_3 and $Cd_{0.04}Zn_{3.96}Sb_3$, respectively. Selected crystallographic details and weight fractions of impurity phases are given in the Supporting Information.

The stoichiometries were refined to $Zn_{37.3(1)}Sb_{30}$ and $Zn_{37.9(1)}Sb_{30}$ for the unsubstituted and the Cd-substituted sample, respectively. This is comparable to the stoichiometries obtained in our previous studies.[25] The lattice constants for the Cd-substituted sample refined to a = 12.2353(1) Å and c = 12.4272(1) Å, and a = 12.2384(1) Å and c = 12.4285(1) Å for the 1 at % Cd sample, which is comparable to the first synthesis batch.

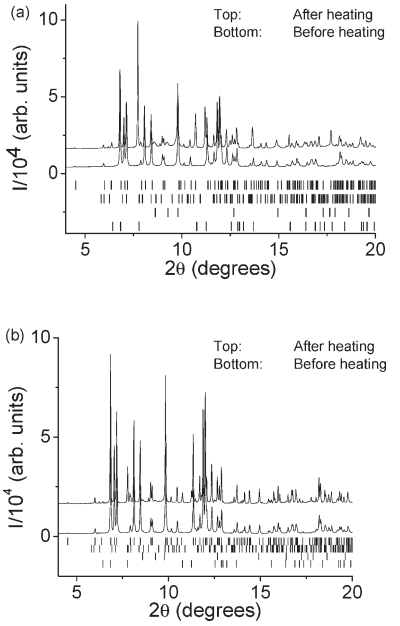

Figure 4. Powder diffraction pattern of (a) the unsubstituted quenched sample and (b) the $Cd_{0.04}Zn_{3.96}Sb_3$ sample before heating (bottom) and after three heating cycles (top), recorded at 300 K. The vertical lines correspond to Bragg positions (from the top) Zn_4Sb_3, ZnSb, ZnO, and Sb, respectively.

Panels a and b Figure 5 show the refined weight fraction of Zn_4Sb_3 and generated impurity phases as a function of temperature for both the unsubstituted and the Cd-substituted sample. The unsubstituted sample starts to decompose below 500 K, and at 500 K the sample has already lost ~4 wt % initial Zn_4Sb_3 phase. The decomposition phases are observed to be ZnSb, ZnO, and Sb. Further heating accelerates the degradation of the Zn_4Sb_3 phase, leaving only ~68% of the original phase at 625 K. Simultaneously, the amount of elemental Sb increases linearly up to almost 20 wt.% at 625 K. At elevated temperatures (575−625 K), large amounts of ZnO is formed, reaching ~10 wt % at 625 K. This corroborates the idea of Zn disappearing from the structure and transforming into ZnO when the compound is heated in atmospheric air.[26] Recent tracer diffusion studies have shown that Zn is highly mobile with properties approaching ionic conductors such as AgI,[27] which explains the disappearance of Zn from the structure. The extreme mobility of Zn in Zn_4Sb_3 may also be the origin of the extreme sensitivity of the thermoelectric properties to the sample compaction method.[28]

(26) Pedersen, B. L.; Birkedal, H.; Frederiksen, P. T.; Iversen, B. B. *Proceedings of the 25th International Conference on Thermoelectrics*; Madeira Island, Portugal, May 9−12, 2006; IEEE: Piscataway, NJ, 2006; p 520
(27) Chalfin, E.; Lu, H. X.; Dieckmann, R. *Solid State Ionics* **2007**, *178*, 447.
(28) Pedersen, B. L.; Birkedal, H.; Iversen, B. B.; Nygren, M.; Frederiksen, P. T. *Appl. Phys. Lett.* **2006**, *89*, 242108.

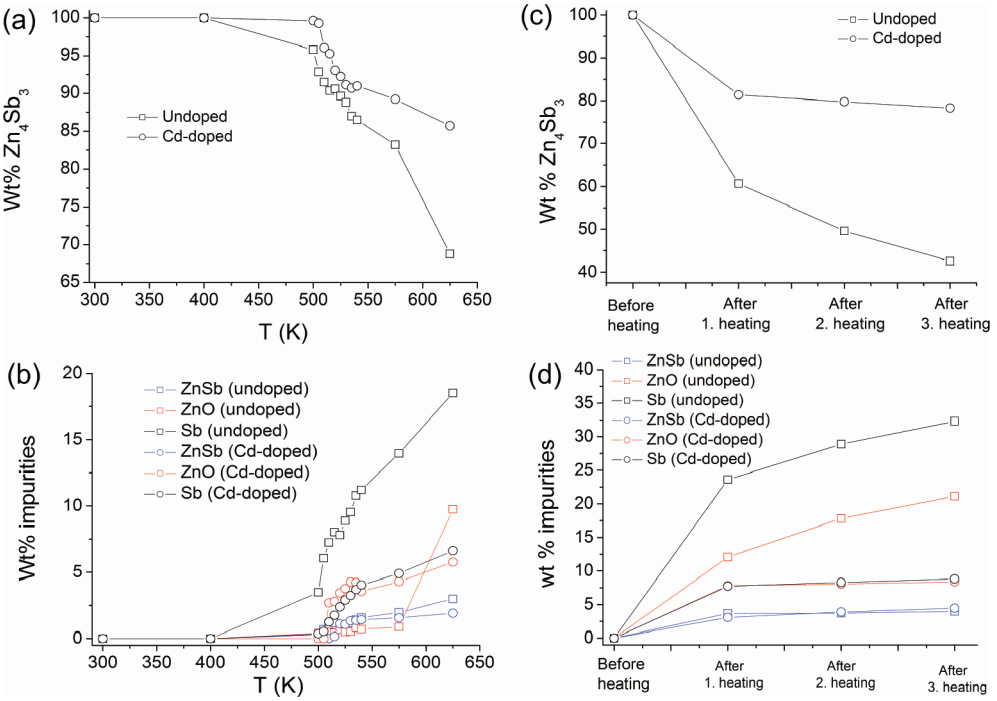

Figure 5. (a) Refined weight fraction of the Zn_4Sb_3 phase as a function of temperature, during the first heating cycle, for unsubstituted and Cd-substituted samples. (b) Refined weight fractions of generated impurity phases (ZnSb, ZnO, and Sb) as a function of temperature, during the first heating cycle. Impurity phases are shown as squares and circles for the unsubstituted and Cd-substituted sample, respectively. (c) Refined weight fraction of the Zn_4Sb_3 phase in unsubstituted and Cd-substituted sample during thermal cycling. (d) Refined weight fractions of generated impurity phases (ZnSb, ZnO, and Sb) during thermal cycling. Impurity phases are shown as squares and circles for the unsubstituted and Cd-substituted sample, respectively.

The Cd-substituted sample has a much higher stability in the first heating cycle (Figure 5a). In contrast to the unsubstituted sample, there is essentially no degradation below 500 K. Between 500 and 540 K, the Cd-substituted sample decomposes with the same speed as the unsubstituted sample, but at higher temperatures the decomposition progresses much slower than in the unsubstituted sample. At 625 K, there is still ~85% of the original phase left, which is a large improvement compared with the ~68% in the unsubstituted sample, and this shows that Cd-doping has a significant effect on the stability. The decomposition of $Cd_{0.04}Zn_{3.96}Sb_3$ generates the same three impurity phases ZnSb, ZnO, and elemental Sb as generated from heating unsubstituted Zn_4Sb_3. However, the formation of ZnO and elemental Sb starts at lower temperatures than in the unsubstituted sample and reaches almost identical levels (~6 wt %) at 625 K.

Panels c and d in Figure 5plot the weight fraction of remaining Zn_4Sb_3 phase and generated impurity phases determined at 300 K after each of the three heating cycles for the unsubstituted and the Cd-substituted sample. Clearly, the unsubstituted sample has a serious stability problem. The sample continues to decompose during cooling from 625 to 300 K and only ~60 wt % remains after the first heating cycle. Repeated thermal cycling causes further degradation, leaving only ~42 wt % of the original phase after three cycles, whereas the rest is decomposed to ZnSb (~4 wt %), ZnO (~21 wt %) and elemental Sb (~32 wt %). Interestingly, the Cd-substituted sample does not seem to degrade further after the first heating cycle. Cooling to 300 K leaves ~81 wt % of the original Zn_4Sb_3 phase and after three heating cycles ~78 wt % still remains. Thus, the Cd-substituted sample appears to reach a stable plateau after a few heating cycles.

It is clear that even 1 at % Cd substitution into the structure has a large effect on the stability of Zn_4Sb_3. Not only is the degree of decomposition significantly smaller during the first heating, but the Cd doping also stabilizes the compound during thermal cycling, which is important for commercial applications. The decomposition of Zn_4Sb_3 produces Zn, which at the surface reacts with oxygen to form ZnO. The stabilizing effect of Cd presumably can be attributed to the bigger and heavier Cd atoms acting as stabilizers to the structure and blocking Zn diffusion. Because all the synchrotron powder diffraction experiments were performed on powders with a small grain size (i.e., large surface area) in atmospheric air, it is conceivable that compacted samples would be more stable during thermal cycling. Furthermore, the stability would most likely be enhanced if the experiments were performed in an inert atmosphere.

Thermal Analysis. Table 2 shows the onset temperatures of the $\beta \rightarrow \alpha$, $\alpha \rightarrow \alpha'$ phase transition for the four samples upon cooling and heating determined by DSC. The calorimetric signatures of the phase transitions are very weak but fully reproducible. The DSC signal as a function of temperature is shown in Figure 6. The unsubstituted sample displays a pronounced peak with an onset temperature of 233 K, which is consistent with the $\alpha-\alpha'$ phase transition temperature at 234 K reported by

Table 2. Onset Temperatures of Phase Transitions Determined by DSC[a]

Cd at %	T_{cool} (K) main	T_{cool} (K) 2nd	T_{heat} (K) main	T_{heat} (K) 2nd
0	233	259	231	252
0.1	234	257	227	254
1	230	no peak	225	no peak
2	226	no peak	223	no peak

[a] Two peaks are expected, one for the $\beta \rightarrow \alpha$ and one for the $\alpha \rightarrow \alpha'$ transition. The main peak has the largest area.

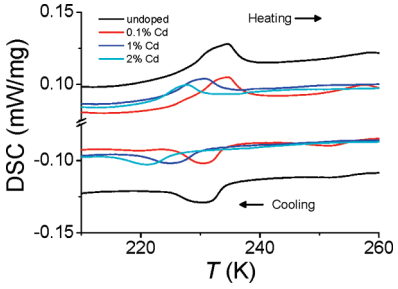

Figure 6. Differential scanning calorimetry signal as a function of temperature for one thermal cycle of both cooling and heating. The signal lines represent unsubstituted Zn_4Sb_3 (black), $Cd_{0.004}Zn_{3.996}Sb_3$ (red), $Cd_{0.04}Zn_{3.96}Sb_3$ (blue), and $Cd_{0.08}Zn_{3.92}Sb_3$ (turquoise).

Mozharivskyj et al.[5] All three Cd-substituted samples show a similar peak, but at slightly different temperatures. The sample containing only 0.1 at % Cd ($Cd_{0.004}Zn_{3.996}Sb_3$) has a peak position almost identical to the unsubstituted sample. Higher doping degrees ($Cd_{0.04}Zn_{3.96}Sb_3$ and $Cd_{0.08}Zn_{3.92}Sb_3$) shift the phase transition toward lower temperatures. Another interesting feature is that the DSC signal becomes smaller with increasing Cd content, which could indicate that Cd-doping has a suppressing effect on the phase transition. This effect has also been noted by other authors in studies where In, Ga and Sn were used as doping elements.[29−31] It has been speculated whether the effect could be explained by the dopant atom substituting on the interstitial Zn sites, because the low-temperature phase transitions are accompanied by ordering of interstitial sites, and substitution on these sites therefore could have a large effect on the phase transition.[30] The relations are the same when heating the samples, e.g., the onset of the phase transition occurs at lower temperatures for the two samples with highest Cd content. All samples have a slight hysteresis around the onset temperature of 2−7 K, compared with the onset temperature upon cooling. Furthermore, the unsubstituted and $Cd_{0.004}Zn_{3.996}Sb_3$ sample displays a weak signal around 257−259 K when cooling the samples. This signal is assigned to the $\alpha \rightarrow \beta$ second-order phase transition, reported at 254 K.[5] The signal was not detectable in the $Cd_{0.04}Zn_{3.96}Sb_3$ and $Cd_{0.08}Zn_{3.92}Sb_3$ samples, which corroborates with the hypothesis of Cd having a suppressing effect on the phase transition. The $\alpha \rightarrow \beta$ phase transition has a hysteresis of 3−7 K.

Physical Properties. All samples used for evaluation of physical properties had a density of more than 97% of the theoretical density (6.39 g/cm^3) as measured on a home-built device based on Archimedes principle. The relative densities are 99% for Zn_4Sb_3, 97% for $Cd_{0.004}Zn_{3.996}Sb_3$, 98% for $Cd_{0.04}Zn_{3.996}Sb_3$, and 100% for $Cd_{0.08}Zn_{3.996}Sb_3$. The physical properties are highly dependent on the sample preparation, and a low sample density or macroscopic cracks will lead to poor performance.[28] We have previously shown that a change in sample density from 90 to 100% can triple the thermoelectric figure of merit for Zn_4Sb_3 samples.[28] Figure 7 shows the Seebeck coefficient as a function of temperature for the four samples. Three of the samples (unsubstituted, $Cd_{0.004}Zn_{3.996}Sb_3$, and $Cd_{0.08}Zn_{3.92}Sb_3$) show a pronounced effect at the phase transition temperature, and they have identical behavior both below and above the phase transition. On the other hand, the phase transition is largely suppressed in the $Cd_{0.04}Zn_{3.96}Sb_3$ sample. The $Cd_{0.04}Zn_{3.96}Sb_3$ sample has poor performance only reaching ~100 μV/K at RT, compared with the other three samples that reach ~140 μV/K at the same temperature. At elevated temperatures, the $Cd_{0.08}Zn_{3.92}Sb_3$ sample seems to perform slightly better than the unsubstituted. Because the $Cd_{0.04}Zn_{3.96}Sb_3$ sample has a high relative density (98%), the relatively poor performance must have another origin.[28]

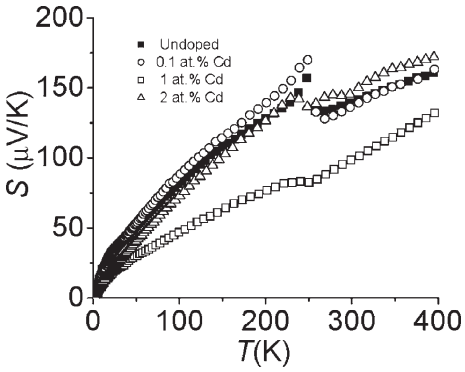

Figure 7. Seebeck coefficient as a function of temperature. The symbols represent unsubstituted Zn_4Sb_3 (full squares), $Cd_{0.004}Zn_{3.996}Sb_3$ (open circles), $Cd_{0.04}Zn_{3.96}Sb_3$ (open squares) and $Cd_{0.08}Zn_{3.92}Sb_3$ (open triangle).

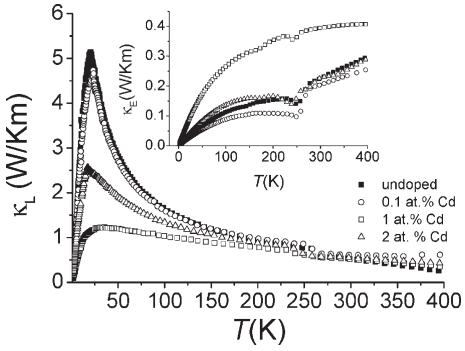

Figure 8. Thermal conductivity as a function of temperature. The symbols represent unsubstituted Zn_4Sb_3 (full squares), $Cd_{0.004}Zn_{3.996}Sb_3$ (open circles), $Cd_{0.04}Zn_{3.96}Sb_3$ (open squares), and $Cd_{0.08}Zn_{3.92}Sb_3$ (open triangle).

The thermal conductivity is shown in Figure 8. In general, the thermal conductivity increases rapidly up to approximately 20 K, where it reaches a peak, and then

(29) Liu, F; Y. Q., X.; Li, D *J. Phys. D: Appl. Phys.* **2007**, *40*, 7811.
(30) Liu, F; Y. Q., X.; Li, D *J. Phys. D: Appl. Phys.* **2007**, *40*, 4974.
(31) Nylen, J.; Lidin, S.; Andersson, M.; Liu, H.; Newman, N.; Haussermann, U. *J. Solid State Chem.* **2007**, *180*, 2603.

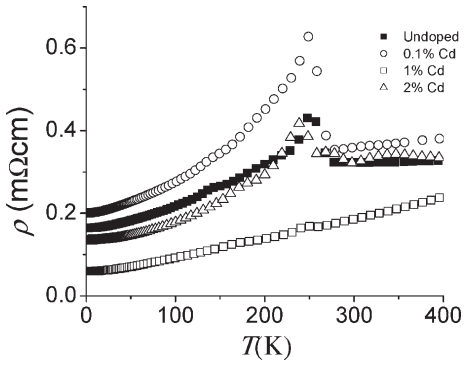

Figure 9. Resistivity as a function of temperature. The symbols represent unsubstituted Zn_4Sb_3 (full squares), $Cd_{0.004}Zn_{3.996}Sb_3$ (open circles), $Cd_{0.04}Zn_{3.96}Sb_3$ (open squares), and $Cd_{0.08}Zn_{3.92}Sb_3$ (open triangle).

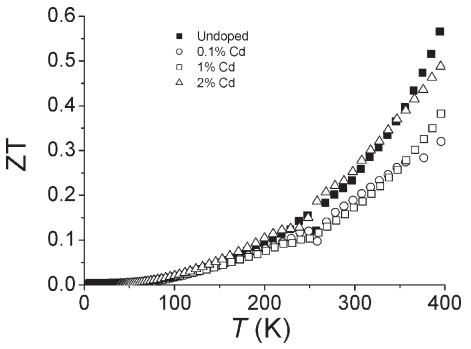

Figure 10. Figure of merit (ZT) as a function of temperature. The symbols represent unsubstituted Zn_4Sb_3 (full squares), $Cd_{0.004}Zn_{3.996}Sb_3$ (open circles), $Cd_{0.04}Zn_{3.96}Sb_3$ (open squares), and $Cd_{0.08}Zn_{3.92}Sb_3$ (open triangle).

falls off as the temperature increases. At low temperatures, the lattice contribution to the thermal conductivity is approximately an order of magnitude higher than the electronic contribution. The unsubstituted and the $Cd_{0.004}Zn_{3.996}Sb_3$ sample have very pronounced peaks, whereas the $Cd_{0.08}Zn_{3.92}Sb_3$ sample displays a peak only reaching half the value of the former samples. The $Cd_{0.04}Zn_{3.96}Sb_3$ sample has essentially no peak at all. We have previously shown that this behavior is an indication of compaction problems and/or changes in the microstructure.[26] The value of all four samples reaches ~0.75 W/Km at RT. At higher temperatures, the unsubstituted sample seems to drop toward lower value, whereas the three Cd-substituted are leveling out and stays at the RT value. It is noteworthy that the phase transition, i.e., ordering of the interstitial atoms has a relatively small effect on κ. Apparently κ is already very low so additional disorder has a minor effect. The resistivity, shown in Figure 9, has a behavior similar to the Seebeck coefficient.

In three of the samples (unsubstituted, $Cd_{0.004}Zn_{3.996}Sb_3$, and $Cd_{0.08}Zn_{3.92}Sb_3$), the phase transition clearly can be seen, whereas the effect is not observable in the $Cd_{0.04}Zn_{3.96}Sb_3$ sample. Furthermore, the $Cd_{0.04}Zn_{3.96}Sb_3$ sample has a very low resistivity compared with the unsubstituted Zn_4Sb_3, both below and above the phase transition temperature. Below the phase transition, the sample containing $Cd_{0.004}Zn_{3.996}Sb_3$ has significantly higher resistivity than the unsubstituted sample, but even though it drops dramatically at the phase transition, the RT level is higher than for the unsubstituted sample. The $Cd_{0.08}Zn_{3.92}Sb_3$ sample has a lower resistivity in the low-temperature phases, compared with the unsubstituted sample, but the two samples display identical values at RT.

The physical properties are summed up in terms of the Figure of Merit in Figure 10. The unsubstituted Zn_4Sb_3 and $Cd_{0.08}Zn_{3.92}Sb_3$ samples show similar behavior and values, reaching ~0.3 at 300 K. At higher temperatures, the $Cd_{0.08}Zn_{3.92}Sb_3$ sample seems to be fading. Both the $Cd_{0.004}Zn_{3.996}Sb_3$ and $Cd_{0.04}Zn_{3.96}Sb_3$ show relatively poorer performance reaching only ~0.2 at 300 K. The density of the $Cd_{0.004}Zn_{3.996}Sb_3$ and the $Cd_{0.04}Zn_{3.96}Sb_3$ samples are 97 and 98%, respectively, compared with 99 and 100% for the unsubstituted and the $Cd_{0.08}Zn_{3.92}Sb_3$ samples, respectively. Although it has been shown that increasing the sample density from 90 to 100% could triple the figure of merit of Zn_4Sb_3,[28] it is not possible to attribute the low-performance of the $Cd_{0.004}Zn_{3.996}Sb_3$ and the $Cd_{0.04}Zn_{3.96}Sb_3$ samples uniquely to this reason in the present work. Differences in microstructure and crystal quality should be taken into consideration as well. The thermoelectric properties of unsubstituted Zn_4Sb_3 and the $Cd_{0.08}Zn_{3.92}Sb_3$ sample are comparable to other reported values at RT.

Conclusion

The influence of slight Cd doping in thermoelectric Zn_4Sb_3 has been investigated. The effect of Cd doping on the phase transition was evaluated by modeling multitemperature synchrotron powder diffraction data, and they revealed that Cd doping has a suppressing effect on the phase transitions and causes them to take place over a larger temperature span than in an unsubstituted Zn_4Sb_3 sample. Furthermore, the individual site occupancies appear to be changed in Cd-substituted samples compared with unsubstituted Zn_4Sb_3 Differential scanning calorimetry suggests a correlation between doping degree and phase transition temperature, i.e., high doping degree shifts the onset temperature toward lower values.

High-temperature synchrotron powder diffraction revealed a significant improvement of the thermal stability of Cd-substituted Zn_4Sb_3, both during initial heating and repeated thermal cycling. In the unsubstituted sample, only ~42 wt % of the original phase is left after three heating cycles to 625 K, compared with ~78 wt % in the Cd-substituted sample. Importantly, the degradation seems to stop in the Cd-substituted sample after the first heating cycle. The decomposition products were identified as ZnSb, ZnO and elemental Sb. Physical property measurements show that although the individual parameters are affected by doping, there is no overall improvement of the thermoelectric performance. On the other hand changes in relative sample density from 97 to 100% appears to have a significant effect on the thermoelectric properties underlining the importance of sample compaction and/or microstructure.

Acknowledgment. The authors gratefully acknowledge the beam time obtained at beamline B2BL02 at SPring8, Japan. Eiji Nishibori and Shinobu Aoyagi are thanked for assistance during data collection. The work was supported by the Danish Strategic Research Council (Centre for Energy Materials), the Danish National Research Foundation (Centre for Materials Crystallography), and by the Danish Research Council for Nature and Universe (Danscatt).

Supporting Information Available: Selected crystallographic details for Zn_4Sb_3, $Cd_{0.04}Zn_{3.96}Sb_3$ and $Cd_{0.08}Zn_{3.92}Sb_3$, derived from rietveld refinement of both the α and the β phase, Tables ST1−ST6; Selected crystallographic details and weight fraction of impurity phases from high-temperature Rietveld refinement of unsubstituted and a 1 at % Cd-substituted sample, Tables ST7 and ST8; Figures S1−S3 plot synchrotron X-ray diffraction patterns for α-phase and β-phase for unsubstituted and Cd-substituted samples, respectively; Figure S4 shows the influence of refinement constraints on Zn occupancy (PDF). This material is available free of charge via the Internet at http://pubs.acs.org.